Temperature-dependent adsorption of hydrogen, deuterium, and neon on porous Vycor glass

T. E. Huber, D. Scardino, and H. L. Tsou
Department of Physics, Polytechnic University, Brooklyn, New York 11201
(Received 10 June 1994; revised manuscript received 15 June 1995)

Adsorption isotherms of H_2, D_2, and Ne have been measured in the temperature range from 15 K to the corresponding critical points in samples of porous Vycor glass. From the Brunauer-Emmett-Teller theory the surface layer coverages are determined. These are found to be temperature dependent. A model-independent approach allows us to fit the data for coverages ranging from submonolayer to thin film, below capillary condensation, for each adsorbate at all temperatures with a temperature-independent curve. This characteristic curve represents the distribution of adsorption sites versus the adsorption potential. In the intermediate coverage range, the isotherms exhibit the modified Frenkel-Halsey-Hill (FHH) behavior. The adsorption saturates for low-adsorption potentials. The characteristic curve is a useful universal curve since it is roughly the same for the three species investigated. We examine the relative strengths of the surface potentials and densities of the two isotopic modifications of hydrogen and of the more classical Ne adsorbed on porous Vycor glass. The characteristic adsorption curve is compared with results from two models for the adsorbate: Dubinin's isotherm for microporous solids and its extension to rough surfaces which places importance on the porosity of the surface, and Halsey's model, which is an extension of the FHH isotherm that takes into account the long-range variations of substrate adsorption potential.

I. INTRODUCTION

Recently, there has been considerable interest in the physics of films of quantum fluids, molecular hydrogen,[1,2] and helium[3,4] on porous substrates. Commercially available porous Vycor glass (PVG) is a prototype absorbent often used in these studies. The adsorption isotherm is the film equation of state. It has long been known that the apparent surface density of helium, as measured by adsorption isotherms, is temperature dependent.[5] Therefore, it is relevant to study the surface densities of hydrogen on this adsorbent to find out if the phenomena is manifest for all light adsorbates. In addition to the interest in light adsorbates as paradigms of quantum behavior, another feature is that their adsorption potentials are the largest, in comparison with the thermal and lateral energies, of any adsorbate. This makes them a suitable testing ground for models of adsorption. We have measured the adsorption isotherms of H_2 and D_2 in the temperature range from 15 K to the critical points, roughly 33 K. Ne was also studied. The Brunauer-Emmett-Teller (BET) method gives surface densities n_{BET} that are temperature dependent for the three gases studied. An early account of these results has been presented.[6,7]

Before discussing the experiments and the application of the characteristic adsorption curve approach to the data, we note that many elements of this model have appeared previously in the literature. The adsorption isotherm is dependent upon the state of aggregation. H_2 adsorption on homogeneous substrates such as MgO is usually interpreted in terms of homogeneous two-dimensional phases or layers. As many as six layers are distinguishable in the adsorption isotherms of H_2 on MgO at low temperatures from many inflection points ("knees") in the plot of material adsorbed as a function of pressure.[2] Adsorbate layers are known to exhibit a hierarchy of structural phase transitions, as recent work on Ar on graphite shows.[8] Also, the strength of the surface adsorption potential "compresses" the adsorbates, in particular helium and hydrogen, leading to an increase of the density of the first adsorbed layer.[9] Another way of increasing the surface density has been proposed in which the energy of a molecule in the second layer is appreciably larger than in the bulk (rather than the model leading to a monolayer, e.g., the BET model).[10] In Steele's model, or the bilayer model, a second layer counts as the surface layer for most measurements, in particular volumetric adsorption measurements. We have previously reported on infrared spectroscopy experiments which seem to favor the bilayer model over the compressed monolayer phase.[11] We have also presented a study of the adsorption isotherms of hydrogen at temperatures between 15 and 20 K for PVG where the adsorption data were analyzed using the bilayer model.[7] In contrast to the BET model, the bilayer model introduces heterogeneity by considering two distinct adsorption energies. From the adsorption data the density and differential adsorption energies of the first two adsorbed layers were determined. Here, we examine a much wider temperature range, the simple picture of two layers breaks down: a model with a wider distribution of adsorption energies is needed in order to fit the data over a wider temperature range.

The characteristic curve aspect of our adsorption data is also a feature of multilayer adsorption theories, such as the Frenkel, Halsey, and Hill (FHH) isotherm.[12] If the long-range part of the gas-solid interaction is due to the

0163-1829/95/52(15)/11372(8)/$06.00

dispersion interaction, the FHH adsorption isotherm is $n = n_{\mathrm{FHH}} \delta\mu^{-\nu}$, with $\delta\mu$ the difference in chemical potential per molecule between saturated and unsaturated conditions and $\nu = \frac{1}{3}$. However, most experimental data for porous materials that have been fitted to a FHH give $\nu = 0.38$ or more.[13] The data presented in this paper can be fitted with a FHH isotherm for intermediate coverages, and values for ν in the high range are also obtained. Following an original suggestion by Halsey, that the discrepancy between theory and experiment can be understood in terms of surface heterogeneity,[14] we have examined the sources of heterogeneity and existing models for heterogeneous adsorption.

When analyzing the problem of adsorption on PVG, several sources of heterogeneity need to be considered. One is the variation in adsorption potential resulting from different microscopic sites in the glass. This compositional disorder has been considered previously.[15,16] Also, geometrical effects can give rise to heterogeneous adsorption over various length scales. Roy and Halsey[17] and Daunt[18] have proposed that the long-range variation of the substrate potential as a function of position on the surface result in islands of adsorbate. This can explain the complex temperature and coverage dependence of the specific heat of helium on heterogeneous surfaces. Tait and Reppy[19] measured the effect for PVG and reviewed the experiments for helium. Torii, Maris, and Seidel[15] have measured the specific heat of hydrogen on PVG and observed similar behavior. They also discussed some possible sources of long-range variation of the substrate potential for H_2. They found that the effect of these heterogeneities is small; for example, the potential at the surface of a 5-nm-diameter spherical pore would be greater than the potential of a flat surface by about 20%. The long-range adsorption potential variations are presumed to give rise to islands of adsorbate in the regions of adsorption potential maxima. We have previously reported on infrared-absorption measurements of the fundamental band of physisorbed hydrogen on PVG which favor the island model of adsorption.[11] Short-range effects are also important. If very small pores exist in PVG which are commensurate with the size of the adsorbent molecules, a strong, short-range heterogeneity follows, since sites of different adsorption energies are possible depending on the position of the molecule about the pore rims.[20]

The field of characterization of porous materials has been renewed by the introduction of the concept of fractal dimension as a measure of surface roughness and morphology.[21,22] Clearly, the number of molecules that overlay a surface at monolayer coverage depends on the linear size r of the probe used, and is $n_M = (S_x/r)^d$, where d is the fractal dimension and S_x is a substrate-dependent prefactor.[23]

The plan of this paper is as follows. In Sec. II we describe the experimental technique and the application of the BET theory to the adsorption data. In this section the adsorption data taken at various temperatures are presented and the adsorption isotherms for H_2, D_2, and Ne are compared. The characteristic isotherms are presented in Sec. III, and their interpretation is discussed in Sec. IV.

II. SAMPLE PREPARATION AND EXPERIMENTS

The experimental technique has been described in detail in Ref. 7. Briefly, the Vycor sample (Corning 7930) consisted of seven rods 3.58 mm in diameter. The total volume was 1.44 ± 0.02 cm^3. It was prepared by boiling in solutions of 30% H_2O_2, rinsing in boiling deionized water, and drying at 150 °C in a vacuum for 2 h. After this process the sample weight was 2.05 g. For hydrogen and neon adsorption measurements the sample was contained in a copper adsorption cell which was mounted in a closed-cycle refrigerator capable of reaching 10 K. Standard N_2 adsorption experiments to evaluate the surface area and average pore size of the Vycor were done by immersing the cell in a liquid N_2 bath. Cell temperatures were measured with a calibrated germanium resistance thermometer. Vapor pressures were monitored with a small (0.5 cm^3) copper cell which was attached to the adsorption cell. The temperature-dependent vapor pressures of H_2 and Ne are given in Ref. 24. Adsorption isotherms were measured by admitting portions of gas from a known volume (453.0 ± 0.5 cm^3) into the adsorption cell through a special valve. This valve internal volume does not change when opening or closing, and allows precise amounts of gas to be admitted into, or removed from, the adsorption cell. Pressures were measured with a temperature-stabilized capacitance gauge.[25] Adsorption cell dead space, that is, space in the adsorption cell not occupied by the porous material, has to be minimized. The volume of the dead space was measured by admitting a charge of helium into the adsorption cell. The reason for using ^{4}He is that it can be assumed to be negligibly adsorbed at 77.4 K. At this temperature, the dead space volume is 0.8 cm^3 at STP. Further corrections, as for the thermomolecular effect, are described in Ref. 7.

The N_2 adsorption isotherm was measured at 77.4 K. The analysis of the data involves fitting the experimental points to the BET equation. From this fit we derive a total internal area of 194 m^2/cm^3. From the measured filling factor of 0.31, and assuming cylindrical pores, a pore radius of 3.2 nm is obtained. These values are consistent with the average pore diameter and porosity given by the manufacturer.

The results for H_2 adsorption are presented graphically in Fig. 1. For clarity purposes, not all the experimental points are shown (although all points were used when analyzing the data). The isotherms are of type IV according to Brunauer's classification,[12] and indicative of a sample with micropores. The isotherms show hysteresis at 18.2 K the saturation pressure is 372 mm hg, the Vycor fills at $x = P/P_0 = 0.82$ and empties at $P/P_0 = 0.63$. The adsorption-desorption loop corresponds to the type of behavior associated with the presence of "ink-bottle" pores or tubular capillaries of variable cross section. Analogous adsorption isotherms for D_2 are shown in Fig. 2.

The BET isotherm may be written as[12,13]

$$\frac{n}{n_m} = \frac{x}{1-x} \frac{c}{1+(c-1)x} , \tag{1}$$

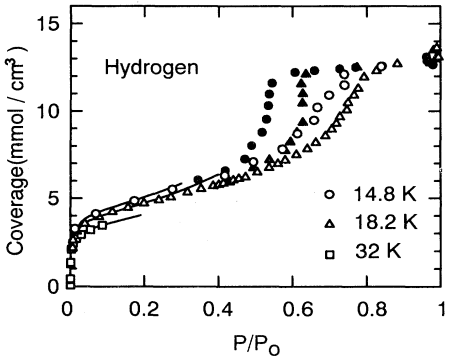

FIG. 1. Adsorption (open symbols) and desorption (full symbols) isotherms of hydrogen. The ordinate axis represents amounts adsorbed per unit volume of the sample. The temperature of the measurements is indicated. P_0 is the saturation pressure at the corresponding temperature. The solid lines represent a calculation based on BET with the parameters of Table I.

where n is the number of moles of gas adsorbed per cm^3 of Vycor at pressure P. x is the reduced pressure P/P_0, with P_0 the saturation pressure; n_m is the number of moles of gas per cm^3 of Vycor sample adsorbed in a monolayer. c is a constant related to the heat of adsorption per mole at the Vycor surface, E_{ads}, and the heat of adsorption per mole E_L at the free surface of the liquid at temperature T:

$$c=(j_1/j_L)\exp[(E_{\text{ads}}-E_L)/k_BT]\ , \tag{2}$$

where k_B is Boltzmann's constant. j_1 and j_L are the partition functions of a molecule in the monolayer and in the liquid, respectively, and they are assumed to be the same.[12]

Since the adsorption isotherms of H_2 and D_2 show hysteresis for high coverages, good fits to Eq. (1) can be obtained only for low coverages. If reduced pressures larger than $x=0.6$ are included, we obtain negative values for c. The value obtained for n_m from the BET fit is rather independent of the saturation pressure, yet larger values

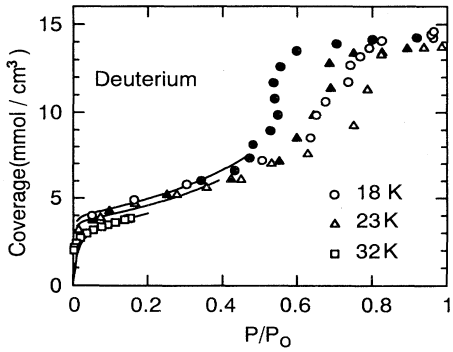

FIG. 2. Adsorption (open symbols) and desorption (full symbols) isotherms of deuterium. The solid lines represent a calculation based on BET, with the parameters of Table I.

TABLE I. Parameters obtained from a fit to the data in Figs. 1 and 2 to the BET equation [Eq. (1)].

	T (K)	n_m (mmol/cm^3)	c
H_2	14.8	4.15	190
	18.2	3.86	160
	32	3.33	210
D_2	18	4	100
	23	3.68	100
	32	3.44	96

are obtained at lower temperatures. The hysteresis loop was also found to be larger at lower temperatures.

The BET fit to the adsorption data for H_2 and D_2 at various temperatures is shown in Figs. 1 and 2. The parameters giving the best fits are listed in Table I. The BET model fits the adsorption data rather poorly. We have shown in Ref. 7 that a modified isotherm based on a bilayer model fits the H_2 data better. Still, the adsorbate density n_m obtained in Ref. 7 is also temperature dependent. Ne adsorption isotherms are qualitatively similar, and also indicate that the adsorbate density is temperature dependent. They are discussed more extensively in Sec. III.

III. CHARACTERISTIC ADSORPTION CURVES

A model-independent approach is discussed which allows us to fit the data for each adsorbate at all temperatures to a characteristic curve. We also discuss the scaling of the adsorption as a function of pressure and temperature with molecular size and mass.

To describe saturation it is convenient to identify a variable that takes temperature into account. A convenient variable is $\delta\mu=\mu_g-\mu_B$, the difference in chemical potential per molecule between unsaturated and saturated conditions. μ_g is the chemical potential per molecule of the gas at temperature T and pressure P. μ_B and P_0 are the chemical potential and vapor pressure of the bulk phase at temperature T. $\delta\mu$ can be calculated from the properties of the gas by using

$$\delta\mu=-T\ln(\rho_0/\rho)+2(B/R)(P-P_0)\ , \tag{3}$$

where R is the gas constant and B is the second virial coefficient.[26] For the gas densities at temperature T and pressure P,ρ, and at temperature T_0 and pressure P_0,ρ_0, we use the virial equation of state. Pertinent data for H_2 and D_2 are presented in Ref. 27. We note that the departure of Eq. (2) from the ideal gas result, $\delta\mu=-T\ln(P_0/P)$, is less than 10%. For neon we use the ideal gas approximation.

When adsorption isotherm data are expressed as a function of the adsorption potential $\delta\mu$, the result is roughly temperature independent for coverages below the hysteresis loop. The thermodynamic meaning of the adsorption potential is discussed in Ref. 28. The chemical potential also has microscopic significance. In the thick-film limit, where the density of the adsorbate is equal to

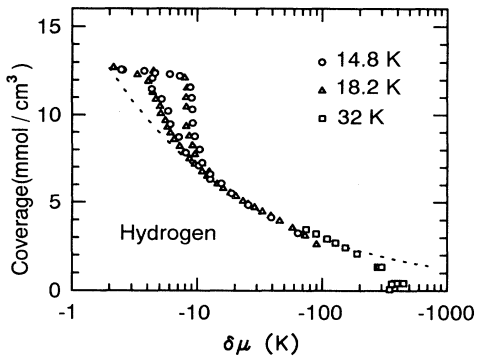

FIG. 3. The characteristic adsorption curve of hydrogen on PVG. $\delta\mu$ is the chemical potential difference between the adsorbed state and the bulk at the same temperature. The dotted line represents a calculation based on the FHH equation, Eq. (4), for $n_{\mathrm{FHH}}=16.41$ mmol/cm^3 and $\nu=0.375$.

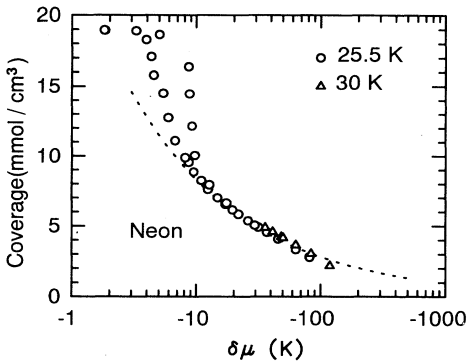

FIG. 5. The characteristic adsorption curve of neon on PVG. The dotted line represents a calculation based on the FHH equation for $n_{\mathrm{FHH}}=24.5$ mmol/cm^3 and $\nu=0.47$.

that of the bulk, and for regular surfaces it can be shown that $\delta\mu=V(z)$, with $V(z)$ the average substrate potential at the gas-adsorbed phase interface. A discussion is given in Ref. 12. The experimental characteristic adsorption curves are shown in Figs. 3, 4, and 5 for H_2, D_2, and Ne, respectively. As shown in these figures, the coverage at various temperatures coalesce into a characteristic adsorption curve $n=n(\delta\mu)$. To a close approximation, a single curve can be obtained at all temperatures. As evidenced by Figs. 3–5, the characteristic adsorption curve concept does not work for coverages and temperatures at which hysteresis sets in; that is, in the region of capillary condensation.

Shown in Figs. 3–5 are the best fits obtained of the FHH equation:[12]

$$n(\delta\mu)=n_{\mathrm{FHH}}(\delta\mu)^{-\nu}, \tag{4}$$

where n_{FHH} is a constant. For hydrogen the best fit is obtained for $n_{\mathrm{FHH}}=16.41$ mmol/cm^3 and $\nu=0.375\pm0.03$. For deuterium the best fit is obtained for $n_{\mathrm{FHH}}=19.32$ mmol/cm^3 and $\nu=0.395\pm0.03$. For Ne we obtained $n_{\mathrm{FHH}}=24.5$ mmol/cm^3 and $\nu=0.47\pm0.06$.

The plots of n vs $\delta\mu$ in Figs. 3–5 show a slight temperature dependence for large adsorption potentials. This is best seen in Fig. 3, the characteristic adsorption curve for hydrogen. Coverages at 32 K are larger than those at 18 K for the same adsorption potential. A similar slight temperature dependence is exhibited by D_2 and Ne. This could be due to a number of reasons. One possible cause is a lack of equilibrium between the adsorbate and pressure gauge. We have repeated the measurements a number of times, and obtained the same results. Surface compression is another effect to be considered.[12] It is important to note here that the compressibility is very different for the three gases studied (being very large for H_2). From the similarity of the characteristic curves, we can infer that the compressibility is not a determining factor in the state of the adsorbed layer.

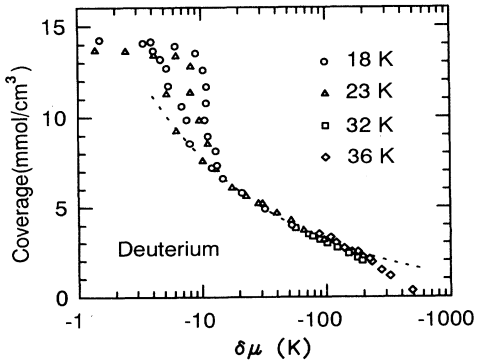

FIG. 4. The characteristic adsorption curve of deuterium on PVG. The dotted line represents a calculation based on the FHH equation for $n_{\mathrm{FHH}}=19.3$ mmol/cm^3 and $\nu=0.395$.

IV. DISCUSSION

In this discussion we consider the BET isotherm, the Dubinin isotherm and its extension to fractal surfaces, and Halsey's interpretation of the modified FHH adsorption isotherm. We also put forward some scaling rules for the characteristic adsorption curves as an aid in relating the adsorption properties of the three gases studied, and as a way of extending the temperature range of applicability of our results. The comparison between adsorption isotherms, n versus P/P_0, of different adsorbates on PVG is arbitrary because the isotherms are temperature dependent. Instead, the scaling of the (temperature independent) characteristic adsorption curve is a powerful predictive tool. It can also be used as a basis for understanding the isotopic and quantum effects of adsorbates in PVG.

An essential feature of the BET isotherm is an inflection, occurring for $\delta\mu=E_L-E_{\mathrm{ads}}$, which identifies the formation of a monolayer in the isotherm. No such inflection is observed in the experimental curves in Figs. 3–5, except for a broad feature at the adsorption potentials, indicating that E_{ads} and n_m are not well defined for the hydrogens and Ne on PVG.

The isotherm equation originally proposed by Dubinin[28] for porous materials turns out to be a better starting point. Dubinin's treatment, as modified by Kaganer,[29] yields a method for calculating the adsorbate density.

This isotherm is confined to the monolayer and submonolayer region. It assumes a Gaussian distribution of adsorption sites on the surface, which can be represented by

$$n = n_K \exp[-\beta(\delta\mu)^2] , \quad (5)$$

with a characteristic adsorption potential $V_K = -\beta^{-1/2}$. Kaganer[29] discussed this equation and interpreted n_K as the number of molecules in a monolayer. Note that the formation of a monolayer, as identified from a bend in the characteristic adsorption isotherm, occurs for $\delta\mu = V_K$. The Dubinin isotherm is useful to describe adsorption on heterogeneous surfaces such as flat (nonporous) glass. Pyrex glass is formed of the same components that constitute PVG and is therefore useful for comparative purposes. We have found that the characteristic curves of hydrogen and neon on Pyrex glass measured by Keesom[30] are remarkably well represented by Eq. (5), for coverages in the monolayer and submonolayer regions. This is shown in Fig. 6 for H_2. Best fits are obtained for $V_K = -135 \pm 15$ K and -79 ± 10 K, for hydrogen and neon, respectively. A modified FHH isotherm with $\nu = 0.38 \pm 0.03$ also fits Keesom's hydrogen data for intermediate coverages.

Equation (5) fits the characteristic curves of Figs. 3, 4, and 5, only over a very limited range of coverages. Best fits are presented in Figs. 7 and 8. The characteristic adsorption potential V_K and the monolayer coverages n_K obtained from the fit to our experimental data are presented in Table II. Note that the characteristic adsorption energies for PVG are larger than for Pyrex. One possible reason for this is that pores have larger adsorption energies than flat surfaces.[15,20] At high coverages, multilayer adsorption occurs, and this is not considered in Dubinin's approach. At submonolayer coverages, in contrast to the adsorption isotherms of H_2 and Ne on flat Pyrex, the adsorption isotherms on PVG are poorly represented by Eq. (5). The low-coverage region will be examined further below.

The relation between n_K and V_K for H_2, D_2, and Ne, shown in Table II, is worth discussing. To explain this relation, in a first approach, one may use rather general molecular and surface properties, without reference to specific statistical mechanics models of adsorption. Hoinkes[31] has presented a simple phenomenological form for the surface potential minimum V_S, $V_S = C\alpha/r_g^3$, where α is the molecular polarizability, C is a constant, and r_g is the molecular radius. Values for the molecular radii and molecular polarizabilities of the relevant molecules are given in Refs. 32 and 33, respectively. We assume that V_K is proportional to V_S. This is validated by the experimental observation that V_K is the same for the

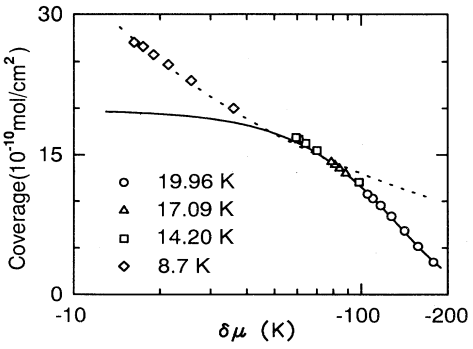

FIG. 6. The characteristic adsorption isotherm of H_2 on Pyrex glass. The data are from Keesom and Schweers (Ref. 30). For clarity, not all experimental points are shown. The solid line represents a calculation based on Dubinin's equation [Eq. (5)] with $\beta = 5.42 \times 10^{-5}$ K^{-2} and $n_K = 19.8$ mmol/cm^2. The short-dashed line represents a calculation based on the FHH equation, Eq. (4), for $n_{FHH} = 85.8$ mmol/cm^2 and $\nu = 0.41$.

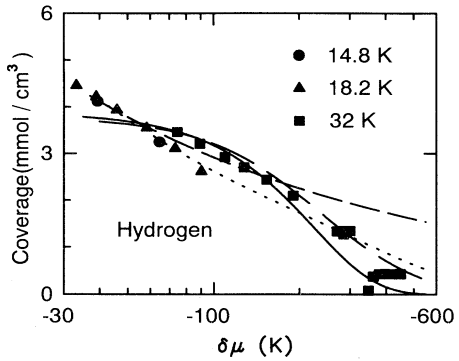

FIG. 7. The characteristic adsorption curve of H_2 at low coverages. The solid line represents a calculation based on Dubinin's equation [Eq. (5)] with $\beta = 2.0 \times 10^{-5}$ K^{-2} and $n_K = 3.88$ mmol/cm^3. The short-dashed line represents a calculation based on the FHH equation. The long-dashed line represents a calculation based on a fractal distribution of micropores, Eqs. (7) and (8), for $x_{min} = 0.2$ nm, $x_{max} = 0.8$ nm, $d = 2.3$, $n_J = 3.8$ mmol/cm^3, and $m = 6.6 \times 10^{-5}$ K^{-2}. The dotted line represents Halsey's isotherm, Eqs. (9) and (10), with $n_H = 3.33$ mmol/cm^3 and $\Delta E_m = 300$ K.

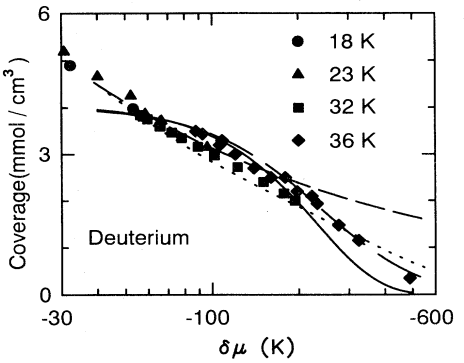

FIG. 8. The characteristic adsorption curve of D_2 at low coverages. The solid line represents a calculation based on Dubinin's equation [Eq. (5)] with $\beta = 1.85 \times 10^{-5}$ K^{-2} and $n_K = 4.08$ mmol/cm^3. The short-dashed line represents a calculation based on the FHH equation. The long-dashed line represents a calculation based on a fractal distribution of micropores, Eqs. (7) and (8), for $x_{min} = 0.2$ nm, $x_{max} = 0.8$ nm, $d = 2.3$, $n_J = 4.2$ mmol/cm^3, and $m = 6.54 \times 10^{-5}$ K^{-2}. The dotted line represents Halsey's isotherm for $n_H = 3.64$ mmol/cm^3 and $\Delta E_m = 300$ K.

TABLE II. Adsorption energy and coverage of the hydrogens and Ne obtained from a best fit of Dubinin's equation [Eq. (5)] to the characteristic isotherms of porous Vycor glass. The neon data do not extend to sufficiently low coverages to allow for a fit of Eq. (5) to the data. Values of V_K and n_K for neon were obtained by scaling the data of deuterium to neon (Figs. 4 and 5).

	V_K (K)	n_K (mmol/cm^3)
H_2	-223 ± 10	3.9 ± 0.1
D_2	-232 ± 10	4.1 ± 0.1
Ne	-90 ± 10	5.5 ± 0.2

two hydrogen isotopes. Hoinkes' expression gives the same result for the two isotopes since they have the same polarizability and molecular radius. For Ne we obtain

$$V_K(\mathrm{Ne})/V_K(\mathrm{H_2})=(\alpha(\mathrm{Ne})/\alpha(\mathrm{H_2}))(r_g(\mathrm{H_2})/r_g(\mathrm{Ne}))^3 =0.60 . \quad (6)$$

This theoretical estimate for the ratio of surface potential minima can be compared with the ratio of characteristic adsorption potentials $V_K(\mathrm{Ne})/V_K(\mathrm{H_2})$ determined from our adsorption isotherms. From Table II we obtain $V_K(\mathrm{Ne})/V_K(\mathrm{H_2})=0.39$, in fair agreement considering that the Ne data do not extend to sufficiently low coverages to allow for a good fit of Eq. (4) to the data. For Keesom's data we obtain $V_K(\mathrm{Ne})/V_K(\mathrm{H_2})=0.58$, in very good agreement with the theoretical estimate.

The adsorption at low coverages and high adsorption energies is very interesting. The formation of a monolayer, as identified from a knee in the isotherm at $\delta\mu=V_K$, is not clearly marked in the data in Figs. 7 and 8. We can consider several explanations for the indefinition of the monolayer in our experimental data. As discussed in Sec. III, this could be from lack of equilibrium of the sample for low coverages, yet experiments were repeated a number of times and the same results were obtained. Another possible explanation is that PVG has a distribution of micropores of different sizes. The effect of a distribution of pore sizes was recently considered theoretically by Jaroniec *et al.*[34] In this case the adsorption isotherm is

$$n(\delta\mu)=n_J\oint_{x_{\min}}^{x_{\max}} J(x)\exp[-mx^2/(\delta\mu)^2]dx , \quad (7)$$

where n_J is the number of moles of gas adsorbed per cm^3 of Vycor. $J(x)$ is the normalized micropore size distribution function, x is the half-width of the slitlike micropores, $x_{\max}$ and $x_{\min}$ denote the maximum and minimum values of x, and m is a parameter related to β. As indicated by Pfeifer and Avnir,[35] the pore size distribution of a fractal surface is

$$J(x)=J_0x^{2-d} , \quad (8)$$

where d is the fractal dimension of the surface, and J_0 is a normalization constant.

As shown in Refs. 36 and 37, the fractal form of the FHH equation [Eq. (4)] can be obtained from Eq. (7) for $x_{\min}=0$ and $x_{\max}=\infty$, with $\nu=3-d$: $n(\delta\mu)=n_{\mathrm{FHH}}(\delta\mu)^{-(3-d)}$. From the fit of Eq. (4) to our intermediate coverage data, an average value of $\nu=0.39\pm0.03$ is obtained for the three gases investigated. We obtain that the fractal dimension of the pore distribution of PVG is $d=2.61\pm0.03$. This has been investigated with other methods, such as small-angle neutron (SANS) and x-ray (SAXS) scattering. The fractal dimension probed by SAXS and SANS refers to surface irregularities in the 1–10-nm length scale, which covers the range probed by adsorption isotherms. Recent SANS experiments give $d=2.4$ for dry samples.[38,39] Analysis of the small-angle x-ray scattering (SAXS) is more involved;[22] a value of $d=2.40\pm0.01$ is obtained from this technique.

We have fitted the isotherm in Eqs. (7) and (8) to our adsorption data at low coverages. Best fits are obtained for a restricted range of pore sizes from $x_{\min}=0.2$ nm to $x_{\max}=0.8$ nm. These fits are shown in Figs. 7 and 8. As shown in Ref. 34 the pore size distribution cannot be unambiguously determined from adsorption data alone. Moreover, we have not been able to fit the entire range of coverages with a single fractal distribution. At low coverages, Jaroniec's treatment suggests a very restricted distribution. However, a much wider pore size distribution, roughly between 1 and 100 nm, is required to fit the intermediate coverages where the FHH works well. Therefore, we were not able to obtain a single distribution that fits at low and intermediate coverages simultaneously. This, coupled with disagreement between the value of d obtained from the modified FHH behavior and previous determinations, leads us to disfavor the fractal form of the adsorption isotherm by Jaroniec *et al.*

We have also fitted the experimental data to Halsey's isotherm for heterogeneous surfaces.[14] This isotherm is based on the assumption that the adsorbate-solid interaction is due to the dispersion interaction and that the distribution of energies over a site in each layer obeys an exponential distribution. Then,

$$n=n_H\sum_{r=1}^{\infty} z^{(r^3)} , \quad (9)$$

where

$$z=(P/P_0)^{T/\Delta E_m} . \quad (10)$$

Here ΔE_m is the modulus of the energy distribution, and n_H is a parameter that adjusts the scale of the number of sites. We assume here that the energy distribution is unrestricted. At intermediate coverages, Halsey's isotherm behaves like a FHH isotherm, Eq. (4), with $\nu=0.37$, independently of the ΔE_m value. Comparison with the experimental data in Figs. 7 and 8 reveals good agreement for intermediate coverages and low energies. Halsey's isotherm fails to fit the data well at low coverages. The discussion of Halsey's theorem can be improved to account for a more realistic distribution of adsorption sites and to reproduce the cutoff for low adsorption potentials, but this is outside the scope of this work.

It is interesting that the isotherms follow a power law at intermediate coverages, and that the same exponent works for hydrogen, deuterium, and Ne on PVG and

nonporous pyrex glass. Furthermore, the molecular masses of hydrogen, deuterium, and neon range from 2 to 22. This indicates that the physical phenomenon that leads to the FHH isotherm is not related to quantum effects. In this context, the study of the temperature dependence of the adsorption of a classical adsorbate such as nitrogen on PVG is of interest. The similarity of the power-law behavior of the characteristic adsorption curves for nonporous and porous glass for intermediate coverages seems to bring further support to Halsey's treatment of the problem. Of course, it could be that the pyrex glass utilized in those studies is microporous. It is conceivable that some surface treatments which induce microporosity were perhaps used, and this should be better investigated.

V. SUMMARY

We have performed adsorption isotherm measurements of hydrogen, deuterium, and neon on porous Vycor glass over a wide temperature range. We find that the BET adsorption isotherm description is unsuitable for this system. We discuss a characteristic adsorption curve approach which can be used to describe the adsorption over wide temperature and coverage ranges. This approach does not work under conditions of capillary condensation, but is very adequate at lower coverages. The temperature-independent characteristic adsorption curve allows for the estimation of adsorption isotherms in the range from submonolayer to multilayer coverages at any temperature in a model-independent way. Overall, the extension of the Dubinin-Kaganer characteristic adsorption curve to heterogeneous surfaces with a pore size distribution of a fractal nature gives the best fits to our data over restricted coverage ranges, but fails to provide a unified picture of the experiments. Also, the fractal dimension obtained from our fits at intermediate coverages is in disagreement with the fractal dimension of the surface of PVG obtained from SAXS and SANS experiments. Halsey's model for heterogeneous adsorption gives remarkably good results considering that it has only two adjustable parameters. In this model, the fluctuations of the adsorption potential are not distributed randomly across the interface, but grouped together so as to give rise to long-range variations of the adsorption potential. These long-range variations can result in large lateral pressures that force the hydrogen to form islands. In this context, our adsorption measurements corroborate the model of adsorption on islands which has been proposed to explain the specific heat of helium and hydrogen on PVG, and which explains some features of the infrared absorption of hydrogen on PVG.

ACKNOWLEDGMENTS

We wish to thank C. A. Huber for helpful discussions. This work was supported by the NSF through Grant No. DMR-926079. Acknowledgment is also made of the Donors of the Petroleum Research Fund, administered by the American Chemical Society, for partial support of this research.

[1]J. L. Tell and H. J. Maris, Phys. Rev. B **28**, 5122 (1983).
[2]J. Ma, L. Kingsbury, F. L. Liu, and O. E. Vilches, Phys. Rev. Lett. **61**, 2348 (1988).
[3]C. Lie-zhao, D. F. Brewer, C. Girit, E. N. Smith, and J. D. Reppy, Phys. Rev. B **33**, 106 (1986).
[4]S. M. Tholen and J. M. Parpia, Phys. Rev. Lett. **68**, 2810 (1992).
[5]For a review, see F. D. Manchester, Rev. Mod. Phys. **39**, 383 (1967).
[6]T. E. Huber and C. A. Huber, in *Fractal Aspects of Materials,* edited by J. H. Kaufman, J. E. Martin, and P. W. Schmidt, MRS Symposia Proceedings No. 20 (Materials Research Society, Pittsburgh, 1990), p. 117.
[7]T. E. Huber and C. A. Huber, J. Low-Temp. Phys. **80**, 315 (1990).
[8]See, for example, J. M. Phillips, Q. M. Zhang, and J. Z. Larese, Phys. Rev. Lett. **71**, 2971 (1993).
[9]S. Francheti, Nuovo Cimento **4**, 1504 (1956).
[10]J. G. Aston and V. R. Mastrangelo, J. Chem. Phys. **19**, 1067 (1951); W. A. Steele, *ibid.* **25**, 819 (1956).
[11]T. E. Huber and C. A. Huber, Phys. Rev. Lett. **59**, 1020 (1987).
[12]For a review of these isotherms see, for example, W. A. Steele, *The Interaction of Gases with Solid Surfaces* (Pergamon, Oxford, 1974).
[13]S. J. Gregg and K. S. W. Sing, *Adsorption, Surface Area, and Porosity,* 2nd ed. (Academic, London, 1982).
[14]G. Halsey, J. Chem. Phys. **79**, 931 (1948); J. Am. Chem. Phys. **73**, 2693 (1951).
[15]R. H. Torii, H. J. Maris, and G. M. Seidel, Phys. Rev. B **41**, 7167 (1990).
[16]T. E. Huber and C. A. Huber, J. Phys. Chem. **94**, 2505 (1990).
[17]N. N. Roy and G. D. Halsey, J. Low-Temp. Phys. **4**, 231 (1971).
[18]J. G. Daunt, Phys. Lett. **41A**, 223 (1972).
[19]R. H. Tait and J. D. Reppy, Phys. Rev. B **20**, 997 (1979).
[20]H. Miyagi, T. Haseda, and T. Nakamura, J. Phys. Soc. Jpn. **54**, 1299 (1985); H. Miyagi, Phys. Lett. **111A**, 187 (1985).
[21]D. Avnir and P. Pfeifer, Nouv. J. Chem. **7**, 71 (1983).
[22]A. Hohr, H. Neumann, P. W. Schmidt, P. Pfeifer, and D. Avnir, Phys. Rev. B **38**, 1462 (1988); A. J. Hurd, D. W. Schaefer, D. M. Smith, S. B. Ross, A. L. Mehaute, and S. Spooner, *ibid.* **39**, 9742 (1989).
[23]H. Van Damme, P. Levitz, F. Bergaya, J. F. Alcover, L. Gatineau, and J. J. Fripiat, J. Chem. Phys. **85**, 616 (1986).
[24]H. H. Mittelhauser and G. Thodos, Cryogenics **4**, 368 (1964); E. E. Yendall, as cited by K. D. Timmerhaus, in *Properties of Materials at Low Temperatures, a Compendium,* edited by V. J. Johnson (Pergamon, New York, 1961).
[25]Baratron pressure gauge Type 127A, MKS Instruments. Through additional temperature stabilization, pressure changes of about 10 Pa over a 24-h period were measured reliably.
[26]C. P. Chen, S. Mehta, L. P. Fu, A. Petrou, and F. M. Gasparini, Phys. Rev. Lett. **71**, 739 (1993).
[27]R. D. McCarty, in *Selected Properties of Hydrogen. NBS*

Monograph 168, edited by R. D. McCarty (U.S. GPO, Washington, D.C., 1981).

[28]M. M. Dubinin, Zh. Fiz. Khim. **39**, 1305 (1965) [Russ. J. Phys. Chem. **39**, 697 (1965)]; B. P. Bering, M. M. Dubinin, and V. V. Serpinsky, J. Coll. Interface Sci. **21**, 378 (1966).

[29]M. G. Kaganer, Proc. Acad. Sci. USSR **116**, 251 (1957).

[30]W. H. Keesom and J. Schweers, Physica V **III**, 1007 (1941); **III**, 1020 (1941).

[31]H. Hoinkes, Rev. Mod. Phys. **52**, 933 (1980).

[32]From J. Hirshfelder, C. F. Curtis, and R. B. Bird, *Molecular Theory of Gases and Liquids* (Wiley, New York, 1954), Table I-A. $\alpha(H_2)=\alpha(D_2)=0.79$ A^3, and $\alpha(Ne)=0.39$ A^3.

[33]From W. F. Edgell, in *Argon, Helium and the Rare Gases,* edited by G. A. Cook (Interscience, New York, 1961). $r_g(H_2)=r_g(D_2)=3.0$ A, and $r_g(Ne)=2.8$ A.

[34]M. Jaroniec, X. Lu, M. Madey, and D. Avnir, J. Chem. Phys. **92**, 7589 (1990).

[35]P. Pfeifer and D. Avnir, J. Chem. Phys. **79**, 3558 (1983); **80**, 4573 (1984).

[36]D. Avnir and M. Jaroniec, Langmuir **5**, 1431 (1989).

[37]P. Pfeifer, J. Kenntner, and M. W. Cole, in *Fundamentals of Adsorption,* edited by A. B. Mersmann and S. E. Scholl (American Institute of Chemical Engineering, New York, 1991), p. 689.

[38]D. Avnir, D. Farin, and P. Pfeifer, New J. Chem. **16**, 439 (1992).

[39]See M. J. Benham, J. C. Cook, J.-C. Li, D. K. Ross, P. L. Hall, and B. Sarkissian, Phys. Rev. B **39**, 633 (1989).